P N P SECONDARY STEAM GENERATOR

thermal power	MJ/s	202
Helium side		
He-flow rate	kg/s	71,1
inlet pressure	bar	40,65
pressure loss	bar	0,54
inlet temperature	°C	750
outlet temperature	°C	203
He-velocity	m/s	17,7
water side		
H_2O-flow rate	kg/s	72
steam outlet pressure	bar	115
pressure loss	bar	6,5
feed-water temperature	°C	150
steam temperature	°C	540
design-data		
inner tube diameter	mm	14,8
outer tube diameter	mm	20
tube length, total	m	76,4
economizer	m	45,0
evaporator	m	22,0
superheater	m	9,4
number of tubes	-	425
heat exchanger surface	m^2	2040
diameter of the inner tube	m	1,2
bundle diameter	m	2,7
bundle height	m	8,43

Fig.9

CONSTRUCTION AND PERFORMANCE TESTS OF A SECONDARY HYDROGEN GAS COOLING SYSTEM

K. SANOKAWA, M. HISHIDA
Tokai Research Establishment
Japan Atomic Energy Research Institute
Tokai-mura, Naka-gun, Ibaraki-ken
Japan

1. Introduction

With the aim of a multi-purpose use of nuclear energy, such as a direct steel-making, an experimental multi-purpose High-Temperature Gas-Cooled Reactor (VHTR)[1],[2] is now being developed in Japan Atomic Energy Research Institute (JAERI). In order to simulate a heat exchanging system between the primary helium gas loop and the secondary reducing gas system of the VHTR, a hydrogen gas loop as a secondary cooling system of the existing helium gas loop was completed in 1977, and was successfully operated for over 2000 hours.

The objectives of constructing the H_2 secondary loop were :

(1) To get basic knowlege for designing, constructing and operating a high-temperature and high-pressure gas facility.

(2) To perform the following tests ;

(a) hydrogen permeation at the He/H_2 heat exchanger (The surfaces of the heat exchanger tubes are coated by calorizing to reduce hydrogen permeation.)

(b) thermal performance tests of the He/H_2 heat exchanger and the H_2/H_2 regenerative heat exchanger

(c) performance test of internal insulation

(d) performance tests of the components such as a H_2 gas heater and gas purifiers.

These tests were carried out at He gas temperature of ∿ 1000°C, H_2 gas temperature of ∿ 900°C and gas pressures of ∿ 40 kg/cm^{2}G, which are almost the same as the operating conditions of the VHTR.

2. Secondary hydrogen gas loop[3]

Figure 1 shows the flow diagram of the secondary H_2 gas loop together with the primary He gas loop. The maximum gas temperature and gas pressure of the H_2 gas loop are 900°C and 42 kg/cm^{2}G respectively.

H_2 gas is circulated by a reciprocating compressor, being heated up to 840°C by a regenerative heat exchanger and a H_2 gas heater. Then it is heated again up to the maximum temperature of 900°C by hot helium gas when flowing through the He/H_2 heat exchanger. The heated H_2 gas is cooled down to a room temperature by the regenerative heat exchanger and a cooler, returning to the compressor. Fluctuations of pressure and flow rate produced by the compressor are absorbed by high- and low-pressure surge tanks.

The temperatures of the H_2 and He gases were measured with W-5Re/W-26Re thermo-couples (The material of the seath is Mo.) or C-A thermo-couples (The materials of the seath are Inconel-600 and SUS 347.), and the surface temperatures of the components by C-A thermo-couples. H_2 gas flow rate was measured with flow nozzles, and He gas flow rate with orifice meters. H_2 and He gas pressures were measured with diaphram-type pressure gauges.

In addition to the main circuit, the secondary H_2 gas cooling system is equipped with a H_2 gas purification system to remove O_2 gas and water vapor, a H_2 gas supply system, a H_2 gas exhaust system to discharge H_2 gas to the atmosphere, a sampling system to analyze O_2 gas and water vapor concentrations in H_2 gas, a N_2 gas protection system and an evacuation system.

A H_2 gas absorber was installed in the primary He gas loop to remove H_2 gas permeated from the H_2 gas loop through the He/H_2 heat exchanger. The H_2 gas absorber consists of a pair of CuO beds as well as a pair of molecular sieve beds.

Main items of the components are presented in Table 1.

3. Test results

3.1 Thermal performance test of the heat exchangers[4]

Figure 2 shows a schematic drawing of the He/H_2 heat exchanger. It is a counter-flow U-type heat exchanger, which consists of five double-tubes. He gas flows inside the inner tubes, and H_2 gas flows in the annular spaces between inner and outer tubes. The tube bundle of five double-tubes in a pressure vessel, and thermal insulation is packed in the space between the tube bundle and the pressure vessel. The H_2/H_2 regenerative heat exchanger is of the same type as the He/H_2 heat exchanger. Main differences of the latter are :

(1) The tube bundle consists of six double-tubes.

(2) No thermal insulation is packed in the lower temperature section.

Table 2 describes the test conditions, and Fig.3 shows a comparison of calculated and experimental overall heat transfer coefficients, which are quite in good agreement.

Figure 4 shows the temperature efficiencies of the He/H_2 heat exchanger. The experimental values are given by the following equations.

$$\left.\begin{aligned} \phi &= \frac{T_{hi}-T_{ho}}{T_{hi}-T_{ci}} \qquad \text{for cooling} \\ \phi' &= \frac{T_{co}-T_{ci}}{T_{hi}-T_{ci}} \qquad \text{for heating} \end{aligned}\right\} \quad (1)$$

The solid lines in this figure are theoretically calculated by the energy balance equations. Temperature efficiencies thus obtained are expressed by

$$\left.\begin{aligned} \phi &= \frac{1}{1-\frac{W_h}{W_c}}\left[\left\{\left(1-\frac{W_h}{W_c}\right)+C_{Loss}\cdot\left(1+\frac{W_h}{K_t\cdot F}\right)\right\}\phi_o - C_{Loss}\right] \text{ for cooling} \\ \phi' &= \frac{1}{1-\frac{W_h}{W_c}}\left[\left\{\left(1-\frac{W_h}{W_c}\right)+C_{Loss}\cdot\left(1+\frac{W_h}{K_t\cdot F}\right)\right\}\phi_o' - C_{Loss}\right] \text{ for heating} \end{aligned}\right\} \quad (2)$$

where ϕ_o and ϕ_o' are the temperature efficiencies when heat loss is ignored, and are given by Eq.(3). C_{loss} expresses the heat loss which is given by Eq.(4).

$$\left.\begin{aligned} \phi_o &= \frac{1-\exp\left\{-\left(1-\frac{W_h}{W_c}\right)\cdot\frac{K_t\cdot F}{W_h}\right\}}{1-\frac{W_h}{W_c}\cdot\exp\left\{-\left(1-\frac{W_h}{W_c}\right)\cdot\frac{K_t\cdot F}{W_h}\right\}} \\ \phi_o' &= \phi_o \times \frac{W_h}{W_c} \end{aligned}\right\} \quad (3)$$

$$C_{Loss} = \frac{Q_{Loss}}{W_c\cdot(T_{hi}-T_{ci})} \quad (4)$$

Where K_t denotes the calculated overall heat transfer coefficient, and Q_{loss} is calculated by $W_h\cdot(T_{hi}-T_{ho})-W_c\cdot(T_{co}-T_{ci})$.

As shown in Fig.4, experimental temperature efficiencies are in good agreement with the values calculated by Eq.(2).

3.2 Performance test of thermal insulation of high-temperature components[5]

In order to keep the temperature of the pressure boundaries below 500°C, thermal insulation is packed inside the pressure vessels of high-temperature components and also inside the pressure tubes of high-temperature pipes. External thermal insulation is placed outside the pressure vessels or tubes of the components excluding the H_2 gas heater and high-temperature He gas pipes. Surface temperature distributions of the pressure vessels and tubes were measured to obtain effective thermal conductivity of insulating materials.

As shown in Fig.2, thermal insulation is packed in a space between the tube bundle and the pressure vessel of the He/H_2 heat exchanger. The internal thermal insulation consists of two layers at the bent section, and three layers at the straight sections. Fibrous thermal insulation mainly made of Al_2O_3 and SiO_2 (Kaowool 1260S) is packed with the density ranging 0.2 ∿ 0.3 g/cm^3 (ε = 0.88 ∿ 0.92). Each thermal insulation layer is separated from the other by a stainless steel foil or pipe. External thermal insulation is 6 mm in thickness.

Figure 5 shows a schematic drawing of a high-temperature He gas pipe connected to the inlet of the He/H_2 heat exchanger. Internal thermal insulation consists of three layers. Fibrous thermal insulation Kaowool 1260S is packed with the same density for He/H_2 heat exchanger. Performance test was carried out under the conditions listed in Table 3. Figure 6 shows circumferential temperature distributions of the pressure vessel of the He/H_2 heat exchanger, and Fig.7 shows those of the high-temperature He gas pipes. All the temperature distributions were not varied by gas pressure and flow rate.

Figure 8 shows effective thermal conductivity of the internal thermal insulation of the high-temperature He gas pipe. The shadowed portion including the curve 1 in this figure represents the range of effective thermal conductivity of Kaowool 1260S measured in He gas environment with high-temperature pipes of similar constructions. The curve 2 indicates the effective thermal conductivity of Kaowool 1260S in He gas converted by the following equation, using the data in air.

$$\lambda_{eff,He} = \lambda_{eff,air} + \varepsilon^{1/3}\cdot(\lambda_{He}-\lambda_{air}) \quad (5)$$

The present data agree well with the curve 2 and also the data reported in references (6) and (7). The measured effective thermal conductivity was kept approximately constant in the pressure range 10 ∿ 40 kg/cm^{2}G.

In a high-temperature and high-pressure atmosphere, Rayleigh number becomes larger because of large temperature difference established across the insulation layer. Consequently natural convection occurs in a horizontal porous medium when the product of Rayleigh number(Ra) and Darcy number(Da) is greater than $4\pi^2$. In a vertical porous medium with one side cooled and the other side heated, however, the effect of natural convection becomes significant at Ra·Da > 1 ∿ 10. When it comes to an annular insulation layer, the occurrence of internal natural convection depends not only on Ra·Da value but also on the ratio of outer to inner radii of the annular section, r_o/r_i.

For example, in the cases when the values of r_o/r_i are 1.25 and 3, the effect of internal natural convection cannot be ignored if Ra.Da are greater than 350 and 10 respectively.

As for the horizontally placed high-temperature components of this loop, the He/H_2 heat exchanger, the regenerative heat exchanger, the He and H_2 gas pipes, r_o/r_i is 1.4 ∿ 1.8 and Ra·Da is smaller than 3, and for the vertically placed H_2 gas pipes Ra·Da is estimated as below 0.01. Therefore the effect of natural convection in the internal thermal insulation of this loop might be not so significant.

The other problems to be considered relating to internal thermal insulation are : the hot spots which might occur at the loose-packing places or the contacting points of spacers, seal plates and supporters with pressure vessels; and the heat losses through the contacting areas. As shown in Figs.6(a) and 7(b), however, the deformations of temperature distribution by the contacting spacers were relatively small, and the estimated heat losses in comparison with total heat loss are ∿ 10% for the heat exchangers as well as He gas pipes, and ∿ 5% for the H_2 gas pipes.

From the above considerations, it could be concluded that there were no defects in thermal insulations as far as the components of the He and H_2 gas loops were concerned.

3.3 Hydrogen permeation test[8]

One of the features of the He/H_2 heat exchanger is that the tube surfaces are coated by calorizing in order to reduce hydrogen permeation. The calorizing by which an aluminum-diffused layer is formed on the surface of metals, has been applied to protect metals from oxidation at elevated temperatures. Few experiments, however, have been done to investigate the effectiveness of calorizing against hydrogen permeation, and all the experiments carried out so far are quite limited to low pressures and relatively low temperatures.[9]

The methods of reducing hydrogen permeation which have been proposed are :

(1) To make an oxide layer on heat tranfer surfaces by adding water vapor in H_2 gas.[10]

(2) By an indirect heat exchanger concept where liquid metal is filled inbetween two heat transfer surfaces.[11]

(3) To make coating on heat transfer surfaces with ceramics, refractory metals, etc..[12]

Calorizing belongs to the category of a method (3). Before applying this calorizing method to the He/H_2 heat exchanger, preliminary experiments were carried out to find what the best combination of base metal and coating is.

Aluminum-powder spraying, calorizing, plasma spraying of zirconia and aluminizing were chosen as the tentative coating methods, and Incoloy-800, HK-40, Inconel-600 and SUS 304 as the tentative base metals. As the experiment proved that the calorized Incoloy-800 was most suitable, the calorizing was employed on the outer heat exchanger tubes of Incoloy-800.

The measured hydrogen permeation rate through the calorized tubes of the He/H_2 heat exchanger was 2 ∿ 3 ℓ(STP)/hour when the average temperature of the tubes was 877°C and the H_2 gas pressure 40 kg/cm^2G. Because the hydrogen permeation rate through the tubes of same base metal without treatment was estimated to be about 100 ℓ(STP)/hour, the reduction by calorizing was tremendous. The reduction factors of hydrogen permeation converted at 1000°C were shown in Fig.9. They were 1/30 ∿ 1/50 and finally remained almost constant during about 1000 hours' operation.

Moreover, the most important thing worthy to note is that the effectiveness of calorizing was neither deteriorated nor dameged by temperature and pressure changes. The calorized layer, as shown in Photo 1, consists of two sub-layers, an Al-rich layer of ∿ 150 μ in thickness and a diffusion layer of ∿ 120 μ in thickness. After the hydrogen permeation test, the tubes were cut and taken out of the He/H_2 heat exchanger to re-examine the calorized layer. General features of the layer were almost the same as before the experiment and no significant defects were observed.

Photo 2 shows a scanning image of the calorized layer taken by an electron-probe X-ray micro-analyzer. A large quantity of Al, Fe, Ni and Cr were observed in the Al-rich and the diffusion layers. It is interesting to note that in the Al-rich layer, those elements were dispersed homogeneously, while in the diffusion layer, Ni, Fe and Cr were distributed in longitudinal ways.

3.4 Performance tests of other components[5]

In Fig.10 the overall thermal efficiency of the H_2 gas heater, which is expressed by the ratio of thermal output to electrical input, was shown. Consequently the net thermal efficiency which is defined by the ratio of thermal output to the heat generated in the element itself excluding in the electrode, junctions, etc. was estimated to be over 80%. The maximum temperature of the element during the operation was 1070°C, which was fairly below the maximum allowable temperature of 1300°C.

Figure 11 shows the results of the performance test of H_2 gas absorber installed in the primary He gas loop. The test was conducted prior to the high-temperature operation, by injecting H_2 gas into He gas flow to measure the H_2 gas concentration at the outlet. The H_2 gas concentration at the outlet could be maintained below 1 p.p.m., except the first switching-over of each CuO bed.

Figure 12 shows the results of the performance test of the H_2 gas purifier. In the test N_2 gas containing O_2 gas as well as water vapor was used. The concentrations of the impurities finally obtained were below 3 p.p.m. at the outlet of the purifier.

4. Summary

A high-temperature and high-pressure hydrogen gas loop which was installed as a secondary cooling system of the existing helium gas loop was successfully run for over 1000 hours under high-temperature and high-pressure operating conditions. The maximum He gas temperature was 1000°C at the inlet of the He/H_2 heat exchanger, and the maximum H_2 gas temperature was 900°C at the outlet, while the maximum He and H_2 gas pressures were 40 kg/cm^2G at the He/H_2 heat exchanger.

Several tests were carried out with this loop, and the results are summarized as follows:

(1) The experimental values of the thermal performance of heat exchangers, such as overall heat transfer coefficient and temperature efficiency, were in good agreement with the calculation.

(2) The temperature distributions of the pressure vessels and tubes of high-temperature components were found to be almost uniform, and no hot spots were observed. Since the effective thermal conductivity of the thermal insulation agreed fairly well with the other data, it could be assumed that no defects in packing occurred.

(3) Hydrogen permeation rate was reduced to 1/30 ∿ 1/50 by calorizing. The reduction rate of hydrogen permeation was not affected by temperature and pressure changes. No defects were observed in the micro-photographs of the calorized layers which were re-examiend after the test. From the above results, it might be said that the calorized diffusion layer is stable in the high-temperature and high-pressure H_2 gas atmosphere, and is quite resistable against the temperature and pressure changes.

The calorizing could be said to be a very promissing method for reducing a large quantity of hydrogen permeation.

(4) The desired performance was achieved with the components, such as the H_2 gas heater, the H_2 gas absorber in the He gas loop and the H_2 gas purifier.

NOMENCLATURE

C_{loss}	:	Defined by Eq.(4).
C_p	:	Specific heat at constant pressure
Da	:	Darcy number
F	:	Heat transfer area of heat exchanger
G	:	Mass flow rate
K	:	Overall heat transfer coefficient of heat exchanger
Q_{loss}	:	Total heat loss from heat exchanger
r_i	:	Inner radius
r_o	:	Outer radius
T	:	Temperature
W	:	C_p X G
ε	:	Porosity of thermal insulation
λ	:	Thermal conductivity
λ_{eff}	:	Effective thermal conductivity of thermal insulation
ϕ	:	Temperature efficiency of heat exchanger for cooling side
ϕ'	:	Temperature efficiency of heat exchanger for heating side

SUBSCRIPTS

air	:	Air
c	:	Low-temperature gas
ci	:	Inlet of low-temperature gas
co	:	Outlet of low-temperature gas
h	:	High-temperature gas
hi	:	Inlet of high-temperature gas
ho	:	Outlet of high-temperature gas
He	:	Helium gas
t	:	Theoretically calculated value

REFERENCES

(1) Murata,H. : Research and Observation Data on Multi-Purpose Use of Nuclear Energy Vol.1, Publication of Fuji International Co.(1973).

(2) Ishikawa,K. et al. : System Design of High-Temperature Gas-Cooled Reactor, Journal of the JSME, 76, 744-782 (1973).

(3) Sanokawa,k. et al. : Experiment on a He/H_2 Heat Exchanger with a High-Temperature and High-Pressure H_2 Gas Loop, (1) Design and Description of the Facility, Preprint of 1977 Fall Meeting AESJ, E 50, 274 (1977).

(4) Takizuka,T. et al. : Experiment on a He/H_2 Heat Exchanger with a High-Temperature and High-Pressure H_2 Gas Loop, (3) Thermal Performance Test of Heat Exchangers, Preprint of 1977 Fall Meeting AESJ, E 53, 276 (1977).

(5) Ogawa,M. et al. : Experiment on a He/H_2 Heat Exchanger with a High-Temperature and High-Pressure H_2 Gas Loop, (4) Performance Tests of Thermal Insulation and Other Components, Preprint of 1977 Fall Meeting AESJ, E 54, 277 (1977).

(6) Suzuki,H. : The Materials of Insulation for Gas-Cooled Very High-Temperature Reactor and Nuclear Steel-Making, Ceramics, 11, 984-993 (1976).

(7) Nakanishi,T. : Completion of High-Temperature Heat Exchanger Test Plant for Research and Development of Nuclear Steel-Making Process, Jounal of AESJ, 21, 147-153 (1979).

(8) Hishida,M. et al. : Experiment on a He/H_2 Heat Exchanger with a High-Temperature and High-Pressure H_2 Gas Loop, (2) Experiment on Hydrogen Permeation, Preprint of 1977 Fall Meeting AESJ, E 51, 275 (1977).

(9) Rudd,D.W. et al. : Permeability of Metals and Enameled Metals to Hydrogen, HAA-SR-6109 (1961).

(10) Röhrig,H.D. et al. : Studies on the Permeation of Hydrogen and Tritium in Nuclear Process Heat Installations, Nucl. Eng. Design, 34, 157-167 (1975).

(11) Sanokawa,K. et al. : A Possibility of Reduction of Hydrogen Permeation Through Heat Exchangers of Multi-Purpose High-Temperature Gas-Cooled Reactor System, Preprint of 1973 Annual Meeting AESJ, C 39, 300-301 (1973).

(12) Flint,P.S. : The Diffusion of Hydrogen Through Metals of Construction, KAPL-659 (1951).

Table 1 Main Items of Components

(1) He/H_2 Heat Exchanger

gas pressure	: 42 $kg/cm^2 \cdot G$
gas temperature ; He in/out	: 1000/860 °C
; H_2 in/out	: 840/900 °C
flow rate ; He / H_2	: 40/30 g/s
tubes ; He side : Incoloy-800, 17.3 ϕ O.D. x 2.3 t	
H_2 side : Incoloy-800, 27.2 ϕ O.D. x 2.9 t	
heat transfer area	: 0.83 m^2
overall heat transfer coefficient	: 720 $kcal/m^2 \cdot h \cdot °C$
pressure tube : AISI 304, 267.4 ϕ O.D. x 9.3 t	

(2) H_2/H_2 Regenerative Heat Exchanger

gas pressure	: 42 $kg/cm^2 \cdot G$
gas temperature ; 1st side in/out	: 883/174 °C
; 2nd side in/out	: 11/720 °C
flow rate	: 30 g/s
tubes ; 1st side : Incoloy-800 & AISI 304, 17.3 ϕ O.D.x 2.3 t	
; 2nd side : Incoloy-800 & AISI 304, 27.2 ϕ O.D.x 2.9 t	
heat transfer area	: 1.78 m^2
overall heat transfer coefficient	: 716 $kcal/m^2 \cdot h \cdot °C$
pressure tube : AISI 304, 216.3 ϕ O.D.x 8.2 t	

(3) H_2 Heater

gas pressure	: 42 $kg/cm^2 \cdot G$
gas temperature ; in/out	: 702/840 °C
flow rate	: 30 g/s
heated element : TZM alloy, 33 ϕ O.D.x1.5 t x 1200 l	
electrode : Mo, 30 ϕ O.D.	
heat transfer area	: 0.113 m^2
pressure tube : AISI 304, 216.3 ϕ O.D.x 8.2 t	

(4) High Temperature Piping

gas pressure	: 42 $kg/cm^2 \cdot G$
maximum temperature	: 900 °C
flow rate	: 30 g/s
flow passage : Incoloy-800, 34 ϕ O.D.x1.65 t	
pressure tube : AISI 304, 165.2 ϕ O.D.x 7.1 t & 139.8 ϕ O.D.x 6.6 t	

(5) Main Compressor

gas pressure	: 42 $kg/cm^2 \cdot G$
flow rate	: 30 g/s
head	: 3 kg/cm^2
rotation frequency	: 350 r.p.m.
stroke	: 130 mm
cylinder	: 110 mm ϕ
moter : 22KW, 6P, 50 Hz, 970 r.p.m.	

Table 2 Test Conditions for Heat Transfer Characteristics of the Heat Exchangers.

(1) He/H_2 heat exchanger

	He gas flow	H_2 gas flow
pressure	20~40 kg/cm²G	20~40 kg/cm²G
flow rate	11~42 g/sec	6.5~28 g/sec
Reynolds number	5000~26000	2400~14000
inlet temperature	400~1000°C	230~860°C
outlet temperature	250~860°C	300~900°C

(2) H_2/H_2 heat exchanger

	hot H_2 flow	cold H_2 flow
pressure	7~40 kg/cm²G	7~40 kg/cm²G
flow rate	6.5~28 g/sec	6.5~28 g/sec
Reynolds number	7900~40000	2800~14000
inlet temperature	300~890°C	5~16°C
outlet temperature	70~170°C	240~720°C

Table 3 Test Conditions for Thermal Performance Test of Inserted Thermal Insulation

—	He/H_2 heat exchanger	He high temp.piping
fluid	H_2	He
pressure	12~41 kg/cm²G	12~41 kg/cm²G
gas temperature	230~900°C	400~1010°C
flow rate	6.5~28 g/sec	11~42 g/sec

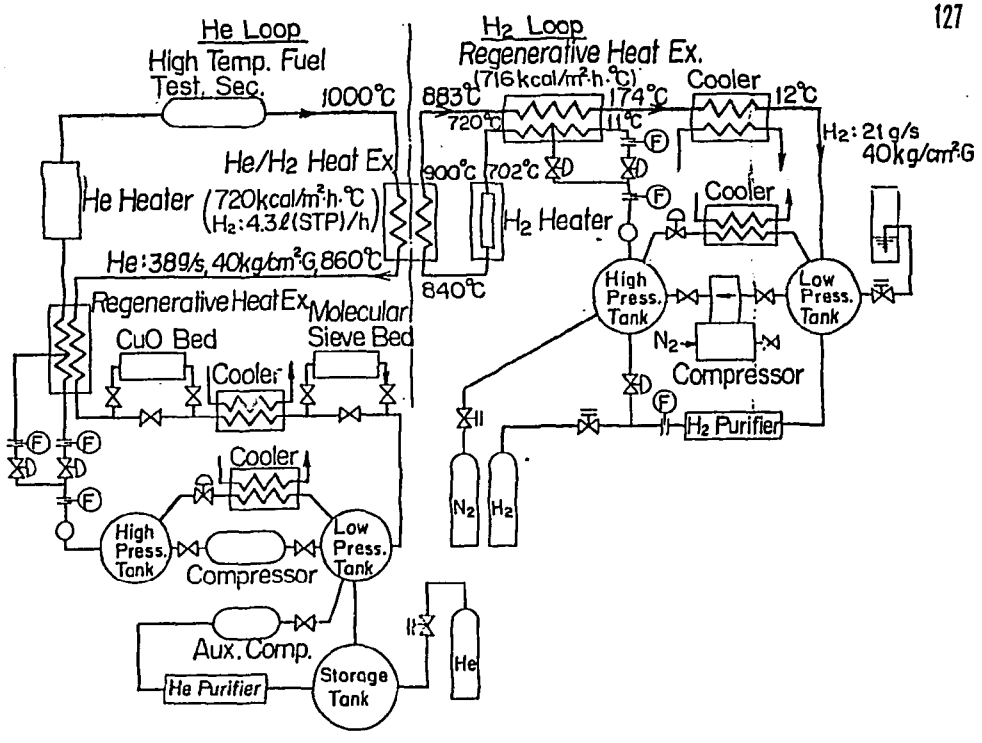

Items	H_2 loop	He loop
pressure	42 kg/cm²·G	42 kg/cm²·G
temperature	900°C	1000°C
flow rate	30 g/s	100 g/s
high temp. pipe	AISI 304 6B / Incoloy-800 1B	AISI 304 8B / Incoloy-800 1B
low temp. pipe	STPA 12-1 B	AISI 304 2B
capacity of heater	50 KW	270 KW

Fig.1 Flow Diagram and Main Items of H_2 and He Loops

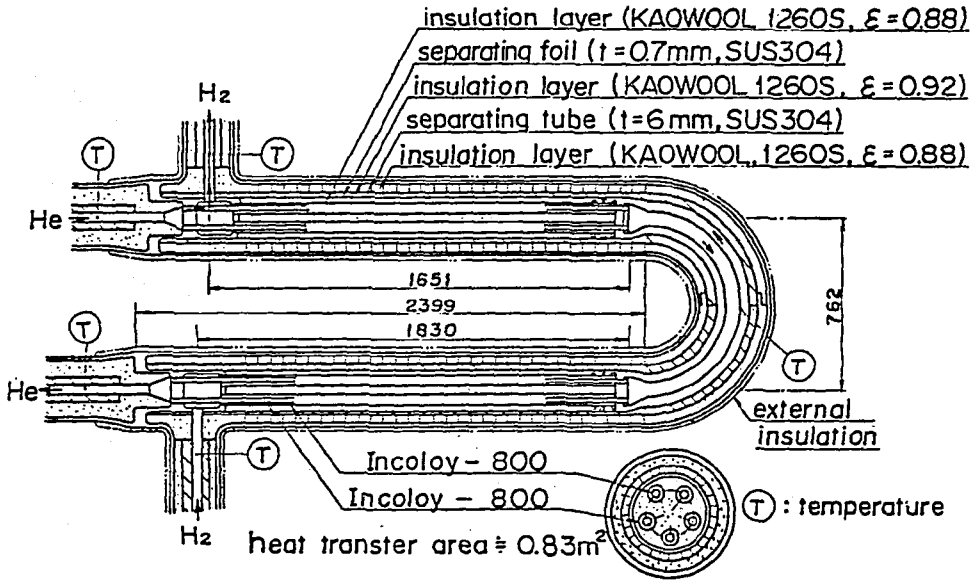

Fig. 2 He/H2 Heat Exchanger

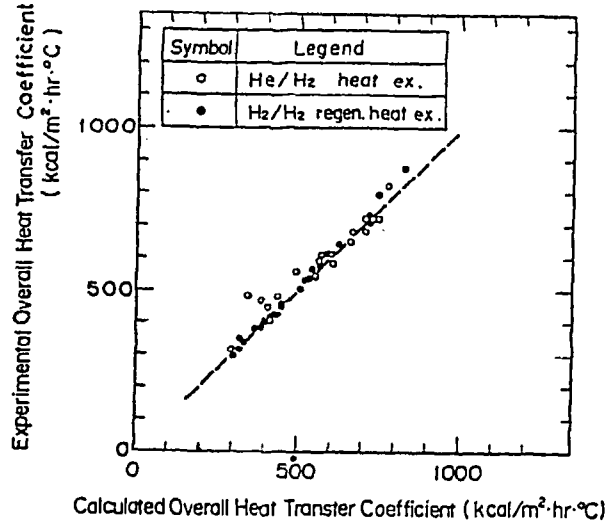

Fig. 3. Comparison of the Experimental Overall Heat Transfer Coefficients with the Calculated Ones.

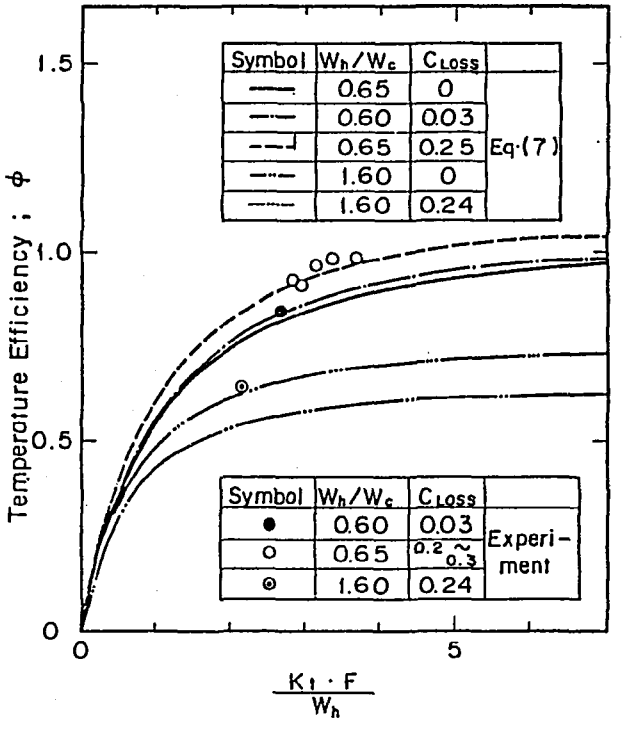

Fig. 4 (a) Temperature Efficiency of He/H_2 Heat Exchanger (He gas side)

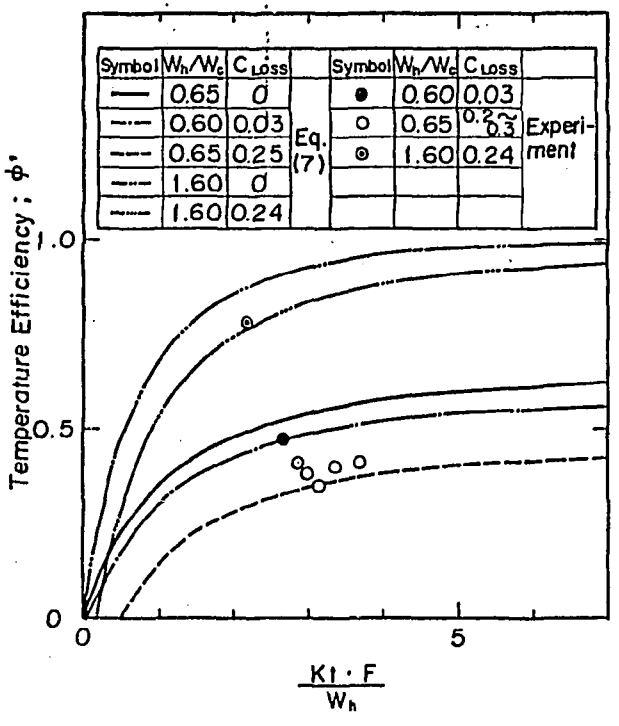

Fig. 4 (b) Temperature Efficiency of He/H_2 Heat Exchanger (H_2 gas side)

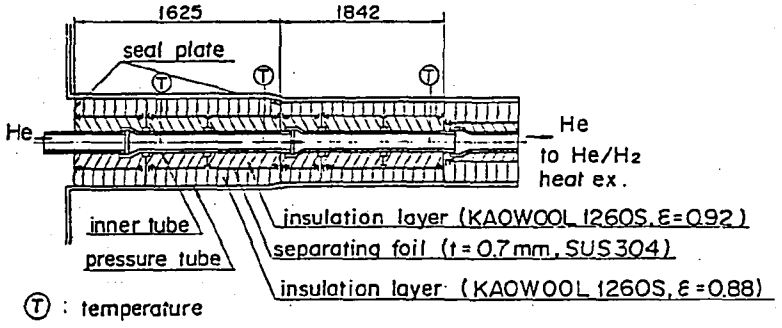

Fig.5. High Temperature Piping System (He gas loop)

Symbol	H_2 temp. (°C)	H_2 press. (kg/cm²·G)
⊙	830 ~ 850	40
⊖	445 ~ 565	40
○	870	8
●	675	40

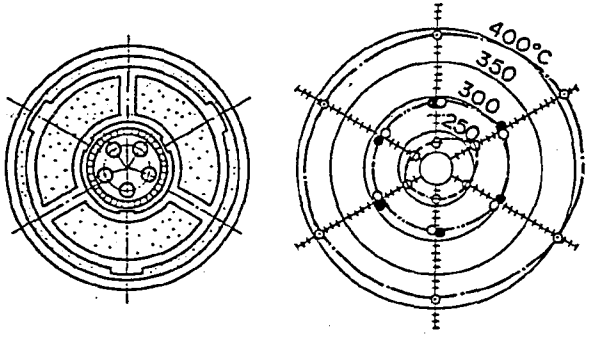

Fig.6(a) Circumferential Temperature Distribution of the Pressure Tube at the Location of a Spacer (He / H_2 heat exchanger)

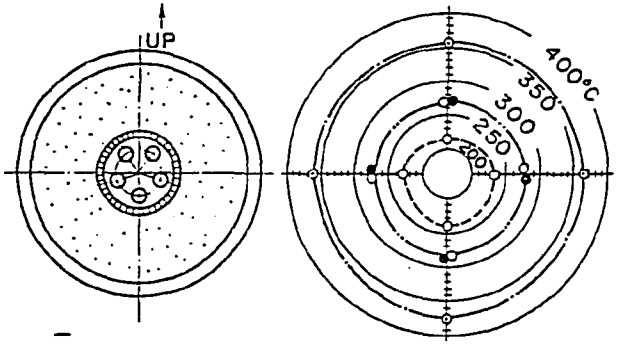

Fig.6(b) Circumferential Temperature Distribution of the Pressure Tube at Normal Locations (He/H_2 heat exchanger)

Symbol	He temp. (°C)	He press. (kg/cm²·G)
⊙	~900	12
○	~570	41
●	~890	41

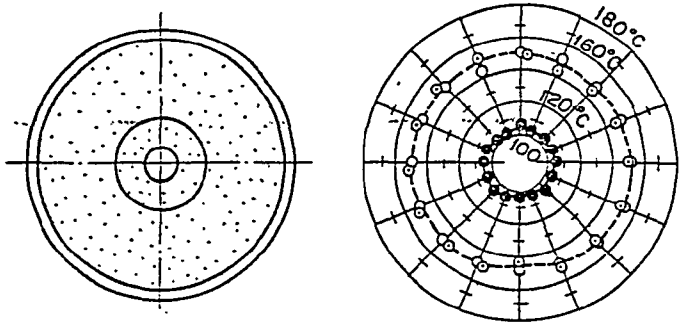

Fig.7(a) Circumferential Temperature Distribution of the Pressure Tube at Normal Locations (He high temp. piping)

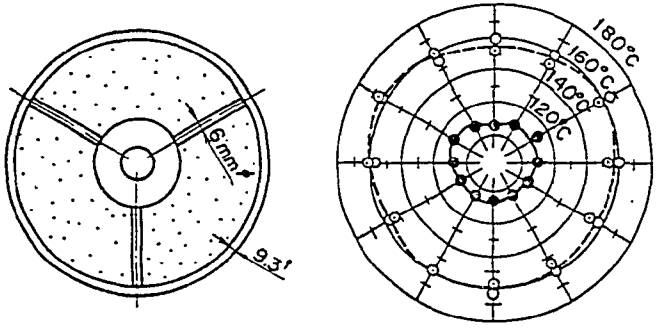

Fig.7 (b) Circumferential Temperature Distribution of the Pressure Tube at the Location of the Spacing Bars (He high temp. piping)

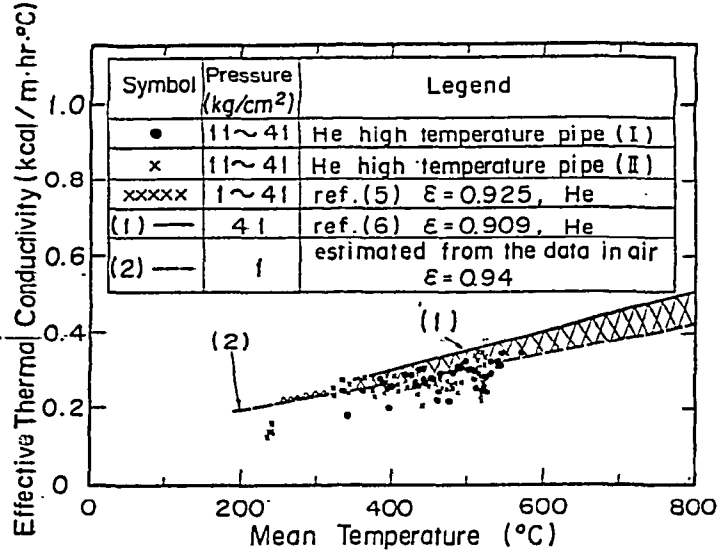

Fig. 8 Effective Thermal Conductivity of Thermal Insulation (KAOWOOL 1260S)

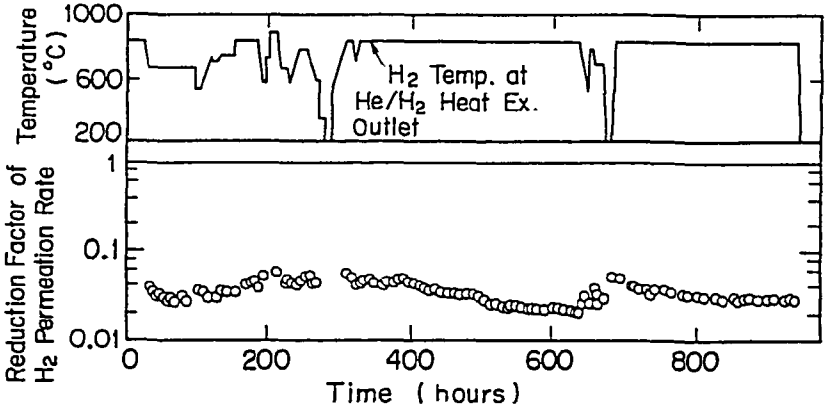

Fig. 9 Reduction Factor of H_2 Permeation Rate

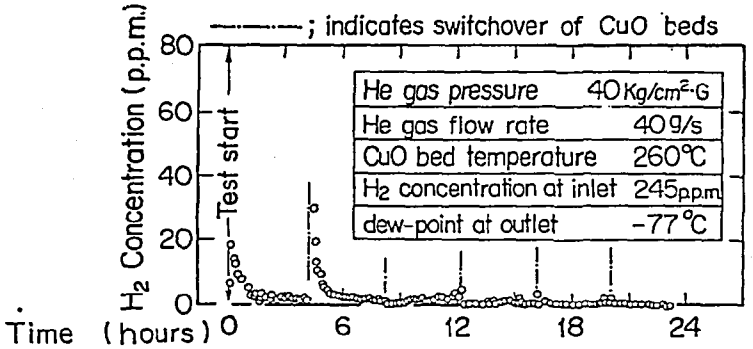

Fig.11 Performance of H_2 Absorber

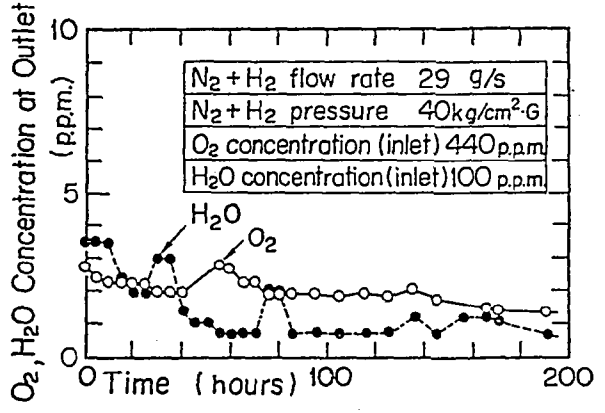

Fig.12 Performance of H_2 Purifier

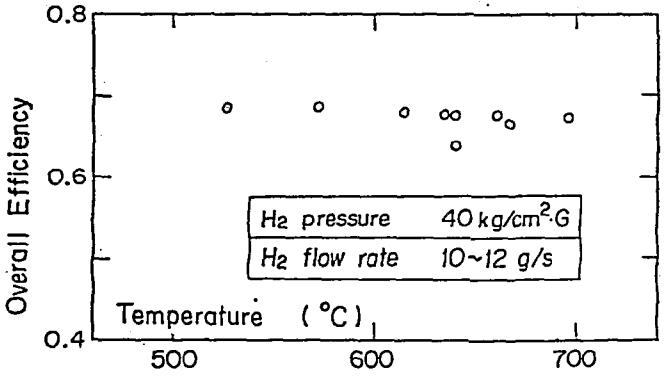

Fig.10 Overall Efficiency of H_2 Heater

A : outer side

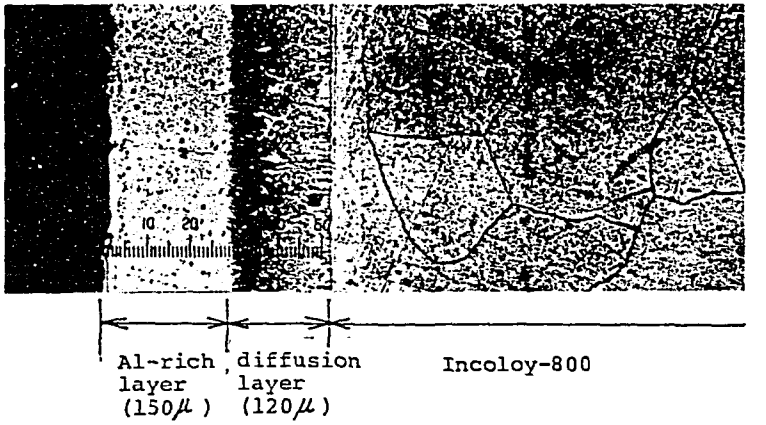

B : middle part

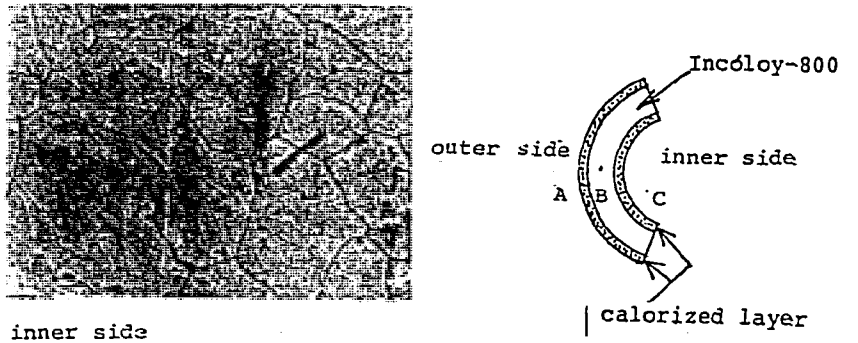

C : inner side

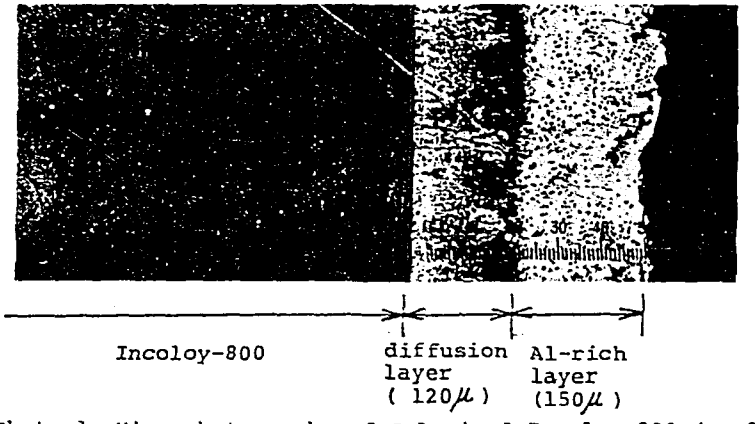

Photo.1 Microphotography of Calorized Incoloy-800 (x 200)

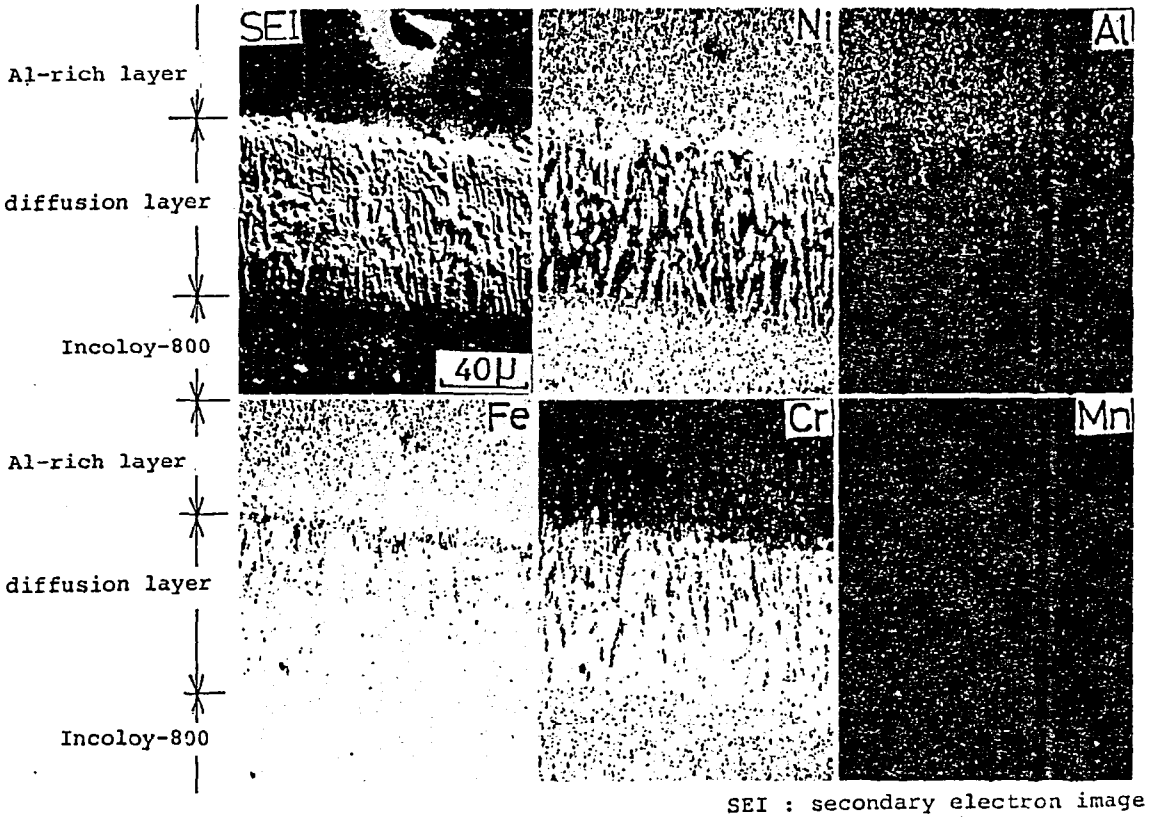

SEI : secondary electron image

Photo.2 Scanning Image by an Electron-Probe X-Ray Microanalyzer

(calorized layer ; outer side of the tube)